

Synergetic Effect of Cationic Starch (Ether/Ester) and Pluronic for Improving Inkjet Printing Quality of Office Papers

Mohit Sharma

University of Coimbra

Roberto Aguado (✉ rag@uc.pt)

University of Coimbra <https://orcid.org/0000-0001-9864-1794>

Dina Murtinho

University of Coimbra

Artur J. M. Valente

University of Coimbra

Paulo J. T. Ferreira

University of Coimbra

Research Article

Keywords: Cationic starch, Paper coating, Pluronic, Printing quality, Starch betainate, Whiteness

Posted Date: June 29th, 2021

DOI: <https://doi.org/10.21203/rs.3.rs-647474/v1>

License:  This work is licensed under a Creative Commons Attribution 4.0 International License.

[Read Full License](#)

1 Synergetic effect of cationic starch (ether/ester) and 2 Pluronic for improving inkjet printing quality of office 3 papers

4

5 Mohit Sharma ^a, Roberto Aguado ^{b,*}, Dina Murtinho ^b, Artur J. M. Valente ^b, Paulo J. T. Ferreira ^a

6

7 ^a *University of Coimbra, CIEPQPF, Department of Chemical Engineering, Rua Sílvio Lima, Pólo II*
8 *– Pinhal de Marrocos, 3030-790 Coimbra, Portugal*

9 ^b *University of Coimbra, CQC, Department of Chemistry, Rua Larga, PT - 3004-535 Coimbra,*
10 *Portugal*

11

12 *rag@uc.pt (Roberto Aguado)

13

14 **Abstract**

15 Improving the printability of paper is still a relevant challenge, despite the fast development of digital communications.
16 While it is well-known that cationic starches enhance ink density, their commercial paper-grade forms are limited to
17 ethers with low degree of substitution. This work addresses the underexplored potential of highly substituted cationic
18 starch for paper coating and its combination with tri-block polymers, namely Pluronic (P123 and F127), taking
19 advantage of their supramolecular interactions with amylose chains. For that purpose, cationic starch ether and ester
20 (starch betainate), both with a degree of substitution of 0.3, were synthesized by alkaline etherification and by
21 transesterification, respectively. Paper without any surface treatment was subjected to one-side bar coating with
22 suspensions encompassing those products and Pluronic, besides other common components. Black, cyan, yellow and
23 magenta inks were printed on all coated papers through an inkjet printer. Key properties of printing quality such as the
24 gamut area, gamut volume, optical density, print-through, inter-color bleed and circularity were measured in a controlled
25 temperature-humidity environment. For instance, a formulation with cationic starch (ether/ester) and P123 improved the
26 gamut area by 16–18% in comparison to native starch-coated paper sheets. Interestingly, the individual assessment of
27 each component showed that cationic starch ether, starch betainate and P123 only improved the gamut area by 5.6%,
28 8.9% and 6.8%, respectively. Finally, but not less importantly, starch betainate was found to quench optical brightening
29 agents to a lesser extent than cationic starch ethers.

30

31 **Keywords**

32 *Cationic starch, Paper coating, Pluronic, Printing quality, Starch betainate, Whiteness*

33 Introduction

34 Paper coating formulations of printing and writing papers (P&W) often comprise a number of different components such
35 as pigments, surfactants, binders, thickeners, dispersants, crosslinkers, optical brightening agents (OBA), and/or
36 lubricants. In each case, the composition depends on which objectives papermakers set for the end product. A careful
37 selection of coating components can therefore be used to develop a paper surface with outstanding smoothness,
38 enhanced barrier properties and, receiving less attention in the literature, improved printing properties (Sharma et al.,
39 2020). Adsorption onto cellulosic fibers occurs when the paper surface is exposed to the coating suspension, but
40 manufacturers cannot neglect the interactions between the components of such suspension, which take place beforehand,
41 from the very moment they are mixed in an aqueous media. These interactions may include competitive adsorption,
42 inclusion complex formation, and stabilization/destabilization (Sousa, De Sousa, Reis, & Ramos, 2014).

43 The inkjet printing properties of fine papers are majorly influenced by the surface properties thereof, such as charge,
44 surface energy, roughness, permeability and surface strength (Bollström et al., 2013). A slight charge on the paper
45 surface may lead to the effective immobilization of the ink pigments onto the coated paper surface, whereas a certain
46 surface energy balance can favor a higher print density (Lundberg, Örtengren, Norberg, & Wågberg, 2010; Stankovská,
47 Gigac, Letko, & Opálená, 2014). Based on that, it has been shown that highly substituted cationic starch (HCS) has a
48 significant positive effect on the ink holdout (Lee et al., 2002), optical density, whiteness, water fastness and ink
49 fathening properties (Gigac, Stankovská, Opálená, & Pažitný, 2016; Lamminmäki, Kettle, & Gane, 2011). These
50 properties, along with the gamut area (GA), further increase in combination with amphiphilic polymers such as
51 poly(vinyl alcohol) (Baptista et al., 2016), most probably due to ease of interpolymer diffusion of ink carriers during
52 printing (Lamminmäki et al., 2011; Sousa et al., 2014).

53 While the biodegradability of native starch is obviously not under question, the biodegradability of its derivatives is too
54 often taken for granted. It has been shown that HCS ethers lose biodegradability with increasing degree of substitution
55 (DS), becoming non-biodegradable at $DS \geq 0.54$ (Bendoraitiene, Lekniute-Kyzike, & Rutkaite, 2018). In this context,
56 starch betainate (SB) rises as a convincing alternative, not only because betaine is naturally found, unlike conventional
57 cationizing reagents, but also because the ester bonds of SB are clearly more labile than ether bonds (Auzély-Velty &
58 Rinaudo, 2003). Likewise, starch betainate (SB), a cationic starch ester, was suggested for the improvement of paper
59 strength since the first work reporting its synthesis (Granö, Yli-Kauhaluoma, Suortti, Käki, & Nurmi, 2000). However,
60 as far as we know, no study has addressed the influence of SB on the printing properties of fine papers. This issue is
61 addressed in the present work, evaluating coating formulations comprising SB and other interesting amphiphilic
62 polymers, namely Pluronics.

63 Pluronics® is BASF's trade name for the less commonly called poloxamers. This trade name comprises non-ionic,
64 water-soluble, triblock copolymers of polyethylene oxide (PEO) and polypropylene oxide (PPO) units. Interestingly
65 enough, they generally form inclusion complexes with starch in aqueous solution. This kind of binding has a significant
66 effect on the dispersion performance and can be explained by hydrophobic interactions between hydrophobic parts of
67 Pluronics® macromolecules and the cavities of the amylose helix (Petkova-Olsson, Altun, Ullsten, & Järnström, 2017).
68 Additionally, the micellar structure of these non-ionic surfactants also influences the adsorption onto the surface of

69 cellulosic materials, which is enhanced in the presence of cationic polymers (Liu, Vesterinen, Genzer, Seppälä, & Rojas,
70 2011; Liu et al., 2010).

71 In light of the aforementioned hypotheses and previous findings, Pluronics was combined with cationic starches in order
72 to observe their effect on the inkjet printing quality parameters. Paper sheets were coated using different concentrations
73 of SB, HCS, Pluronics (P127 and F127), precipitated calcium carbonate (PCC), alkyl ketene dimer (AKD) and optical
74 brightening agent (OBA). This study also illustrates the use of a statistical tool to design the coating experiments and to
75 identify the most important factors to be considered for improving the paper printability. A comparison of HCS and SB
76 coatings was also explored, discussing their influence on the whiteness of paper, given that the interaction between
77 cationic polymers and OBAs, generally anionic, has been pointed out as a major cause of fluorescence quenching (Shi et
78 al., 2012).

79

80 **Materials and Methods**

81 **Materials**

82 Native corn starch (NS), α -amylase (in standard buffer solution, pH 5.8), PCC, OBA and AKD were of industrial origin.
83 3-Chloro-2-hydroxypropyltrimethyl ammonium chloride (CHPTAC), Pluronics® P123 (MW \sim 5750 g mol⁻¹, PEO \sim 30
84 %wt. and CMC of 0.313 mM at 20 °C) (Alexandridis, Holzwarthf, & Hatton, 1994) and Pluronics® F127 (MW
85 \sim 12600 g mol⁻¹, PEO-70 %wt. and CMC of 0.56 mM at 25 °C) (Thapa, Cazzador, Grønlien, & Tønnesen, 2020) were
86 purchased from Sigma-Aldrich. Betaine hydrochloride (99%) was purchased from Alfa Aesar and used as-is for
87 transesterification. All solvents were purified or dried prior to use the standard procedures. Other commercially available
88 compounds were used without further purification.

89

90 **Synthesis of HCS and SB**

91 Native starch was mildly hydrolyzed with α -amylase (0.45 μ L g⁻¹ of starch), under continuous stirring, at 80 °C for 5
92 min. The temperature was raised up to 90–95 °C for 15 min. Then, the starch solution was cooled down and absolute
93 ethanol was added to precipitate the polysaccharide, hereinafter referred to as “cooked starch”. Cooked starch was then
94 vacuum filtered, dried and stored in an oven at 50 °C. This pretreatment is common to the synthesis of both HCS and
95 SB.

96 HCS was synthesized as described elsewhere (Haack, Heinze, Oelmeyer, & Kulicke, 2002). Briefly, 10 g of cooked or
97 native starch was converted into HCS using 33.5 mL of CHPTAC (60% wt.) and 5.9 g of NaOH. The reaction was
98 carried out for 24 h at 70 °C in 100 ml of distilled water. The reaction mixture was then neutralized with a 0.1% HCl
99 solution.

100 Starch betainate (SB) was synthesized, as described in a previous paper (Sharma, Aguado, Murtinho, Valente, &
101 Ferreira, 2021), through the transesterification of starch with methyl betainate (MeBetCl) in polar aprotic solvents. 24 g
102 of betaine hydrochloride was first esterified to synthesize MeBetCl using 11.3 mL of thionyl chloride and 75 mL of

103 methanol, under reflux, for 4 h at 70 °C. MeBetCl was recovered through evaporation of methanol followed by
104 trituration in diethyl ether and, finally, the crude product was dried under high vacuum. Then, 10 g of starch were
105 converted into SB using 20.8 g of MeBetCl in *N,N*-dimethylformamide (DMF), 100 mL. Prior to transesterification,
106 cooked starch was pre-activated in NaOH/ethanol. The reaction was carried out for 24 h at 70 °C.
107 HCS and SB were precipitated by adding ethanol (alcohol/water > 10, v/v), vacuum filtered and washed with absolute
108 ethanol, followed by drying at 50 °C.

109

110 **Characterization of synthesized cationic starches**

111 Attenuated Total Reflectance-Fourier Transform Infrared (ATR-FTIR) spectroscopy, ¹H-nuclear magnetic resonance
112 (¹H-NMR) spectroscopy and viscometry analysis were performed to characterize the synthesized cationic starches.
113 ATR-FTIR spectra were recorded by using an Agilent Cary 630 spectrometer, from 750 to 3000 cm⁻¹, at a resolution of
114 4 cm⁻¹ and 64 scans per sample. NMR spectra were obtained from a Bruker Biospin GmbH spectrometer, at 400 MHz,
115 using D₂O as solvent. The degree of substitution was calculated from the area of the singlet assigned to the methyl
116 protons of the quaternary ammonium group. The reliability of this result was confirmed by measuring the nitrogen
117 percentage of samples on a Fisons Instruments EA 1108 CHNS-O elemental analyzer.

118

119 **Paper coating**

120 NS was used as a common component for preparing all formulations in this work. For that, NS was cooked as described
121 earlier, and then cooled down to 50 °C instead of precipitated. An industrial calendered uncoated paper (base paper, BP),
122 produced from bleached eucalyptus kraft pulp with a basis weight of ~ 78 gm⁻², was used as substrate for performing
123 surface coating.

124 Coating of BP was performed using a Mathis laboratory coater, with a pre-drying infrared system coupled to the
125 applicator bar (SVA-IR-B). An applicator roll with the diameter of 0.13 mm, in conjunction with a velocity of 6 m min⁻¹
126 and intermediate load at both sides, was used to achieve 1.5 to 3 g m⁻² per side, on the basis of dry coating weight.
127 Coated paper sheets were air dried at room temperature.

128 Besides NS, BP sheets were coated with SB, HCS, P123, F127, PCC, and combinations thereof. Coatings were
129 performed using 8%, 16% and 24% of total solids coating weight of each of these components, and several combinations
130 of them were tested at said concentrations. The coating compositions resulting from individual components (with NS)
131 and combinations thereof are shown in Table 1 and 2, respectively.

132 The surface weight gain was calculated by the difference between basis weights (ISO standard 536:1995) of the air-dried
133 coated paper sheet and the respective BP sheet. Before characterization, all coated papers were kept at controlled
134 temperature (23 °C ± 1) and humidity (RH 50% ± 2). For each run, three numbers for paper sheets were coated and
135 characterized for evaluating the printing quality.

136

137

138 Table 1. Composition of coating components expressed as %w/w, on the basis of dry coating weight.

Ingredients	Coating formulations													
	HCS/SB				P123			F127			PCC			Reference
HCS/SB	8	16	24	16										
P123					8	16	24							
F127								8	16	24				
PCC											8	16	24	
OBA	6	6	6		6	6	6	6	6	6	6	6	6	6
AKD	0.4	0.4	0.4	0.4	0.4	0.4	0.4	0.4	0.4	0.4	0.4	0.4	0.4	0.4
NS	85.6	77.6	69.6	83.6	85.6	77.6	69.6	85.6	77.6	69.6	85.6	77.6	69.6	93.6

139

140 Table 2. Composition of coating components for the interaction study, expressed as %w/w, on the basis of dry coating weight.

Ingredients	Coating formulations										
	HCS/SB +P123					HCS/SB +P123+PCC					Reference
HCS/SB	16	16	16	16	16	16	16	16	16	16	
P123	8	16	24	16		8	16	24	16		
PCC						16	16	16	16		
OBA	6	6	6			6	6	6			6
AKD	0.4	0.4	0.4	0.4	0.4	0.4	0.4	0.4	0.4	0.4	0.4 0.4
NS	69.6	61.5	53.6	67.6	67.6	53.6	43.6	37.6	51.6	51.6	93.6 99.6

142

143 Statistical analysis

144 In order to observe the interactions between coating components and their impact on the printing quality of coated
 145 papers, JMP software was used as a statistical tool for the design of experiments and data analysis. In this study, four
 146 continuous factors, namely HCS, P123, PCC and OBA, were selected, each at two levels (0 and 16%), and a full
 147 factorial design with two center points was chosen to design the coating experiments. A total number of 18 runs were
 148 performed to evaluate the effect of these factors and their ternary interactions on the printing quality, namely: GA; OD
 149 for cyan, magenta, yellow, and black; PT; inter-color bleed (ITCB), and circularity for black color in the responses.

150

151 Printing quality

152 The printing quality was evaluated as reported elsewhere (Lourenço, Gamelas, Sarmiento, & Ferreira, 2020). Briefly, the
 153 coated papers were printed using HP Officejet Pro 6230 inkjet printer, having cyan, magenta, yellow, and black color
 154 ink cartridges. The printed sheets were air dried for 4 h under controlled conditions of temperature and humidity.

155 The GA is the area of the hexagon resulting from the a* and b* coordinates of six printed colors (red, green, blue, cyan,
 156 magenta, and yellow), where a* axis represents the color from green to red and axis b* represents the color from blue to
 157 yellow. It was determined by measuring the values of CIE L*a*b* coordinates for six color spots, including three base
 158 colors (cyan, magenta and yellow) and other three complimentary colors (red, green and blue). For that, the “X-Rite Eye
 159 One XTreme UV Cut” spectrophotometer was placed on each printed color spot, activating the UV light (D50, 2°). The

160 readings were taken in the sequence of red, green, blue, cyan, magenta, and yellow color spots. Additionally, CIE
 161 $L^*a^*b^*$ values for black and white colors were measured to estimate the gamut volume (GV) of printed paper sheets.
 162 In order to evaluate the other printing properties, such as OD and PT, the QEA PIAS-II spectrophotometer was used
 163 with a low resolution optical module (33 μ m/pixel with visual area of 21.3mm \times 16mm), along with the software PIAS
 164 II, based on ISO 13660 quality standards, for processing the images. The PT of a printed paper requires the measurement
 165 of $L^*a^*b^*$ values on the opposite side, in contrast with the non-printed area of the same paper sheet. The transmitted
 166 light intensity from a specific area of each color (black, white, cyan, magenta, and yellow) was measured using QEA
 167 PIAS-II, and thus PT and OD were calculated from the following equations:

168
$$\text{Optical density} = \text{Log}_{10}(\text{Insident light}/\text{Transmitted light}) \quad \text{Equation 1}$$

169

170
$$\text{Print through} = \sqrt{(L_p^* - L_u^*)^2 + (a_p^* - a_u^*)^2 + (b_p^* - b_u^*)^2} \quad \text{Equation 2}$$

171 where L^* , a^* , b^* are the CIE chromatic coordinates, and the subscripts u and p refer to areas of unprinted and back of
 172 the printed black spot, respectively.

173 The other printing properties, namely ITCB and circularity (black), were also evaluated by means of QEA PIAS-II with
 174 high resolution module (5 μ m/pixel with 3.2mm \times 2.4mm). This was used to measure the raggedness, which can be
 175 defined as the geometric distortion of the line and dots, given by the standard deviation of the residue from the lines and
 176 dots adjusted to their ideal limit. The higher the raggedness, the worse the ITCB and circularity.

177

178 Paper properties

179 The surface hydrophilicity for SB-coated papers was evaluated by contact angle goniometry. The static water contact
 180 angle (WCA) was measured in an OCA 20 goniometer (Dataphysics, Germany) using the sessile drop method. A droplet
 181 of deionized water (10 μ L) was automatically poured onto the coated paper surface. After settling, the formed angle was
 182 measured by fitting the Young-Laplace equation to the drop profile. Bendtsen roughness (ISO 5636-3, 8791-2) and
 183 Gurley air permeability (ISO 5636/5) were also measured for coated papers using appropriate testers from Flank.
 184 Whiteness (CIE W D65/10) of coated papers was measured using D65 illumination in the Elrepho spectrophotometer.
 185 The average value and the standard deviation of four independent measures are reported for CA, Bendtsen roughness,
 186 Gurley air permeability and whiteness. This last property was related to the performance of OBA, as fluorescence
 187 emission spectra of solutions containing OBA were recorded by means of a FluoroMax 4 spectrofluorometer from
 188 Horiba.

189 The kinematic viscosity was determined using a size 100 Cannon-Fenske viscometer in a thermostatic bath (TAMSON
 190 TV 2000) set at 40 $^{\circ}$ C. Measurements followed the ISO 3105 standard. Polymer solutions were prepared with a
 191 concentration of 5 mg cm^{-3} in 1M NaOH/H₂O (for HCS) and DMSO (for SB). The thermogravimetric analysis (TGA)
 192 was carried out on a thermo-microbalance TG 209 F3 Tarsus, from Netzsch Instruments. Samples were heated from 40
 193 $^{\circ}$ C to 600 $^{\circ}$ C, under a flow of nitrogen (20 mL min^{-1}), with a heating rate of 10 $^{\circ}$ C min^{-1} . TGA was performed for filter

194 paper coated with P123, F127 and SB. A filter paper was cut into pieces (5cm × 2 cm) and Pluronics P123/F127 were
195 absorbed in this cellulosic substrate. This was carried out with a 10% Pluronic aqueous solution and a LayerBuilder dip
196 coater from KSV. Cellulose substrates were dipped into the solution for 3 min, pulled out and air-dried. The same
197 procedure was followed for 10% SB and 10% P123/F127 + 10% SB aqueous solutions.

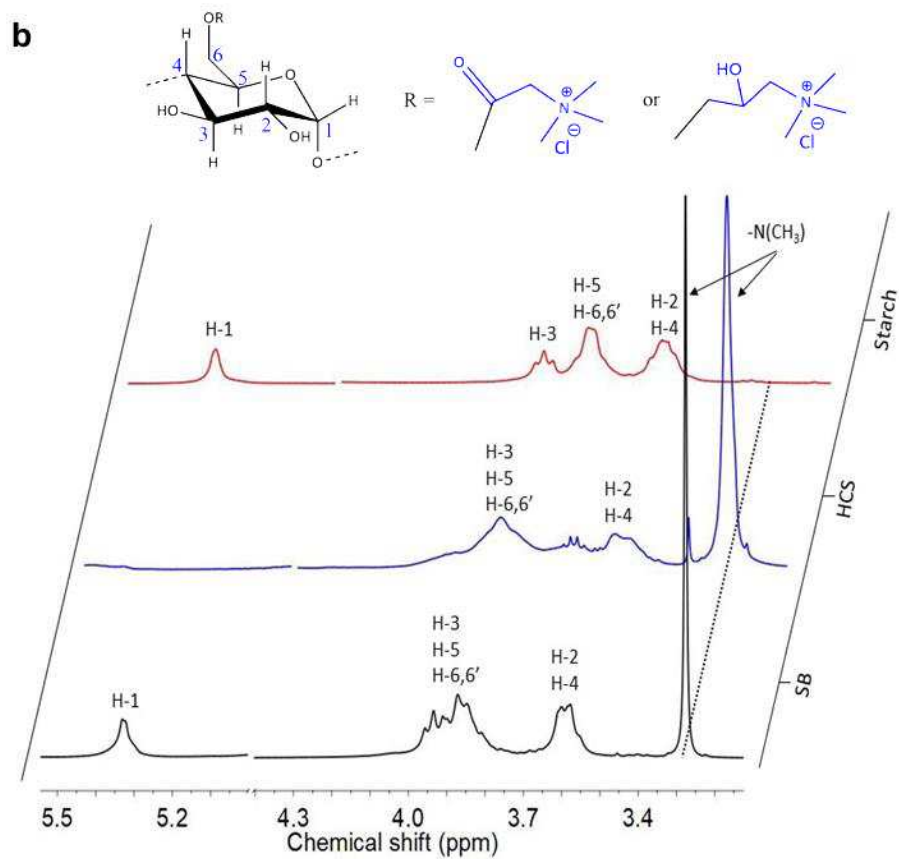
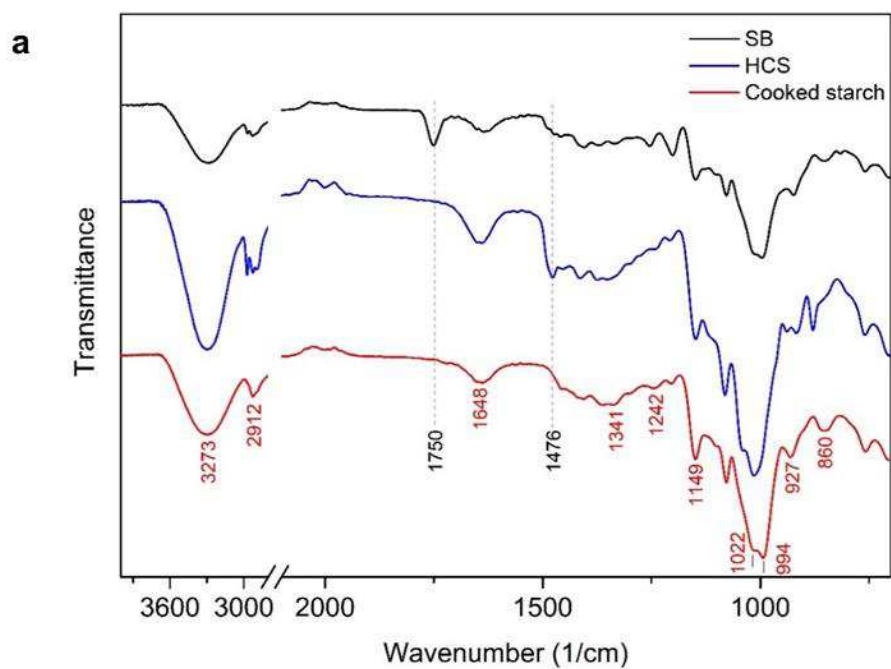
198

199 **Results and discussion**

200 **Synthesis of SB and HCS**

201 Figure 1a presents the ATR-FTIR spectra for synthesized cationic starches from etherification and transesterification,
202 using respectively CHPTAC and betaine hydrochloride, in comparison to the NS spectrum. The absorption peaks at
203 3300 cm^{-1} , 2912 cm^{-1} , 1648 cm^{-1} can be assigned to the $-\text{OH}$, $-\text{CH}_2$ stretching vibrations, and H_2O bending vibration
204 due to water sorption, respectively. Additionally, peaks at 994 cm^{-1} can be attributed to the ether bonds and the
205 absorption band at 897 cm^{-1} can be assigned to C1–H bending in starch. Compared to cooked starch, a new prominent
206 peak at 1473 cm^{-1} can be observed due to the quaternary ammonium group attached to the anhydroglucose unit (AGU)
207 (Hebeish, Higazy, El-Shafei, & Sharaf, 2010; Wang & Cheng, 2009). Furthermore, the absorption band at 1750 cm^{-1} is
208 assigned to the ester bond in SB.

209 Figure 1b shows the $^1\text{H-NMR}$ spectra for HCS and SB, compared to the spectrum of cooked starch. The singlet at 3.28
210 ppm is assigned to the nine hydrogens of methyl groups of the quaternary ammonium. The resonances from 3.5 to 4 ppm
211 represent the hydrogens attached to carbons 2, 4, 5, 6 (H-6 and H-6'), and 3 of AGU, typically in that order. The doublet
212 for the H-1(α) anomeric proton lies downfield (5.35 ppm). There was a certain shift upfield and broadening of all signals
213 upon cationization. No impurities were detected in SB, but the HCS spectrum displayed a singlet at 3.33 ppm and a
214 quadruplet at 3.65 ppm, none of which belong to the canonical structure of cationic starches. The former could be due to
215 quaternary ammonium groups arising from substitution on hydroxypropyl chains, instead of the hydroxyl groups of
216 AGU.



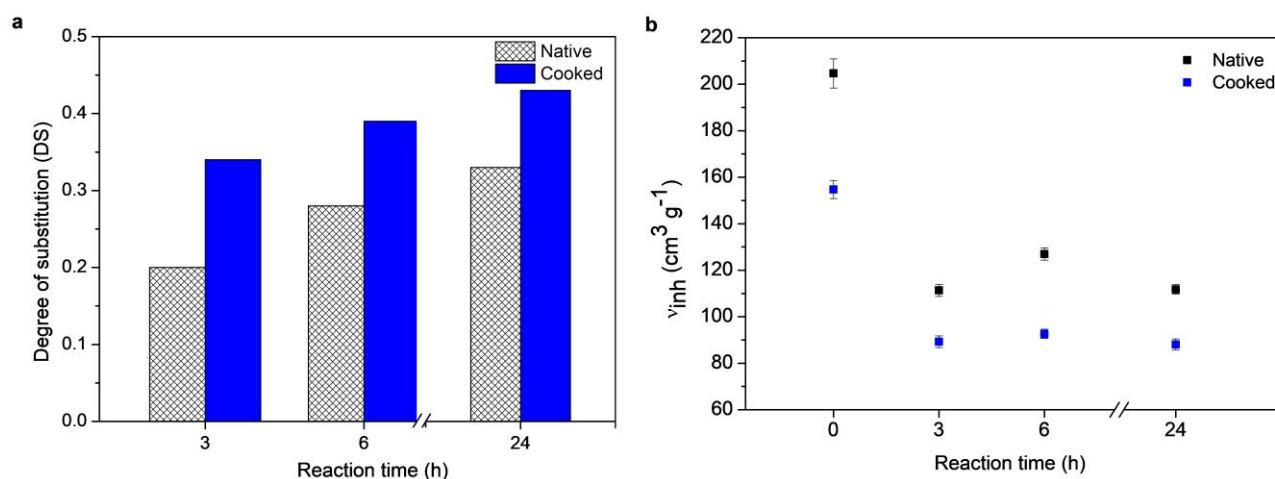
218

219 Figure 1 ATR-FTIR (a) and ^1H -NMR (b) spectra for cationic starch ether and starch betainate, compared to cooked
 220 starch.

221

222 An important hypothesis regarding the reaction is that enzymatic cooking improves its efficiency. Figure 2a shows the
 223 effect of cooking and reaction time on the DS of the synthesized HCS. It can be observed that the DS increases from
 224 0.20 to 0.33 and from 0.34 to 0.43 with the increase in the reaction time from 3 to 24 h, when native and cooked starches
 225 were used as raw materials for the etherification reactions, respectively. This is likely due to the formation of more
 226 porous starch granules, which facilitates the access of the reagent to hydroxyl groups (Huber & BeMiller, 2001). It was
 227 also observed that the cooking of starch enables the homogeneous dispersion of starch granules in the solvent by
 228 increasing the solubility and decreasing its viscosity, as seen in Figure 2b (Gao, Luo, Fu, Luo, & Peng, 2012).

229 Undoubtedly, due to the cleavage of 1–4 α -D-glucopyranosyl linkages of amylose and amylopectin, the inherent
 230 viscosity decreases with the enzymatic pre-treatment, from 199.4 $\text{cm}^3 \text{g}^{-1}$ (NS) to 151.8 $\text{cm}^3 \text{g}^{-1}$ (cooked starch). The
 231 viscosity was further reduced by 43–45% when using them in etherification. Likewise, the hydrolysis of starch
 232 molecules in highly alkaline media and at high temperature is evidenced by a loss of viscosity after functionalization.
 233 Nonetheless, after reaction times beyond 3 h, further hydrolysis is either negligible or compensated by the effects of
 234 cationization on polymer-solvent interactions.



235
 236 Figure 2 Effect of reaction time and enzymatic cooking on degree of substitution (A) and inherent viscosity (B) of HCS.

237
 238 Like etherification, the increase in DS and decreasing in viscosity were also observed in the synthesis of SB. However,
 239 DS increased much more abruptly, from 0.01 to 0.33, when using NS and cooked starch in the transesterification
 240 reaction, respectively, proving the poor reaction efficiency with NS. Given that the inherent viscosity decreased by
 241 ~73%, starch faced higher depolymerization during functionalization, mostly due to the previous alkalization of starch at
 242 high temperature.

243 Paper printing properties

244 Both native starch and CS require cooking before adding other coating components to prepare a uniform coating
 245 solution. It should be noted that the other coating components (PCC, Pluronic, OBA and AKD) were always added
 246 after cooling down the starch solution to 50 °C. It should be stressed that the P123 and F127 have critical micelle
 247 concentrations of 0.313 mM (20°C) and 0.56 mM (25°C), respectively. These values are lower than the amount of

248 Pluronics used in the experiments reported here; additionally, the critical micelle temperatures of these surfactants are
249 well below 50 °C which also support that Pluronics are in the micelle form (He & Alexandridis, 2018).

250 In order to prepare the coating formulations, corn native starch was used as host component and cooked using α -
251 amylase enzyme in aqueous medium at 80 °C, for 5 min. CS was then added and cooked together with native starch at
252 90-95 °C for 15 min. The starch solution was cooled down for 15 min.

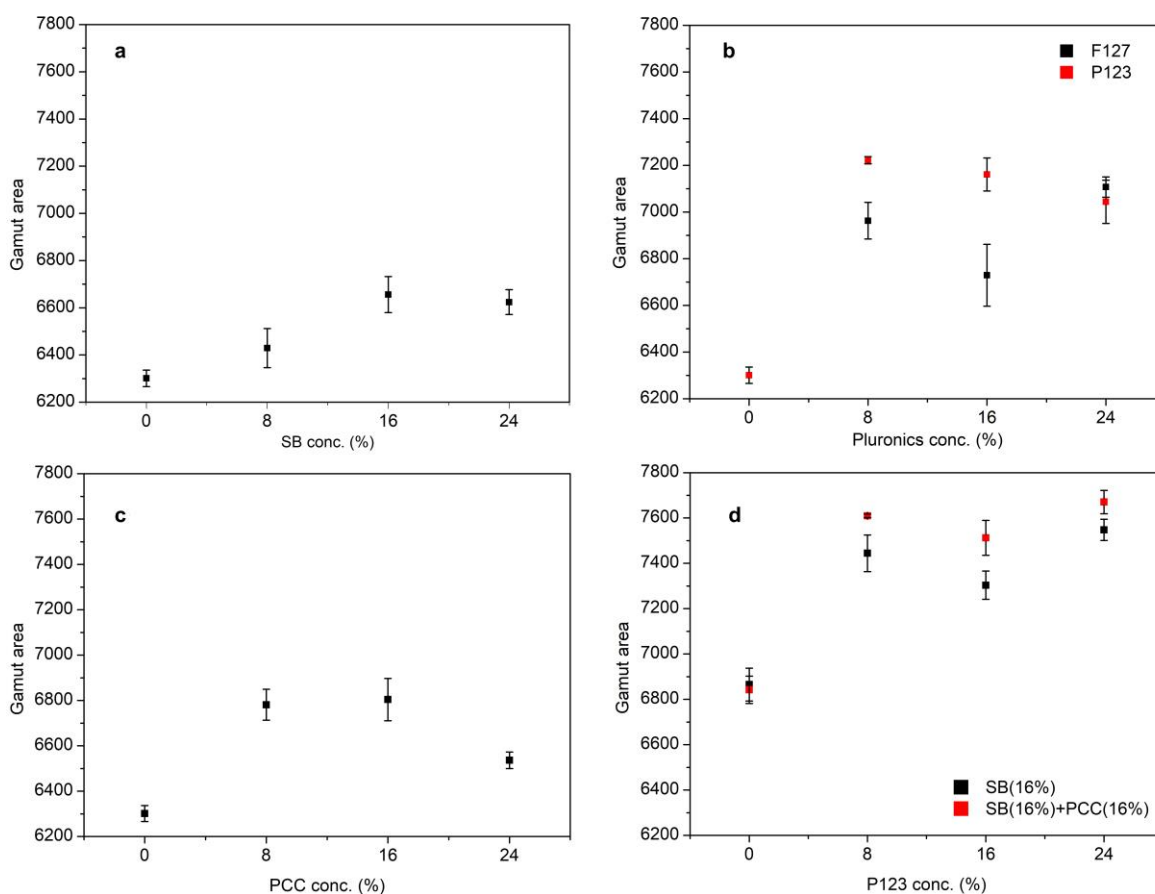
253

254 Gamut area

255 It was observed that the GA, presented in Figure 3a, increased by 8.6%, 9%, and 12.5% using 8%, 16% and 24% dry
256 solids content of SB, respectively, compared to NS coating. Plausibly, the high DS led to higher deposition of SB on the
257 paper surface, resulting into improved GA (Niegelhell et al., 2018).

258 Besides charge density, addition of SB slightly increased the hydrophobicity of the paper surface and smoothness; both
259 also contributed to improve GA (Gigac, Stankovska, & Pazitny, 2016) (Gigac, Stankovska, et al., 2016). Table 4 can be
260 referred to for the Bendtsen roughness, and contact angle values for SB coated papers.

261 Similarly to GA, GV, which considers the color luminance L, besides a and b, also increased with increasing SB
262 concentration. The maximum increase was observed as 16.4% using 24% of SB, compared to NS coating (refer Table
263 4).



264

265 Figure 3 Effect of different concentrations of SB (a), Pluronics (b), PCC (c), and their combinations (d) on GA.

267 Table 3 Properties of coated papers using different concentrations of SB, Pluronic (P123 and F127), and their
 268 combination in coating formulations.

	Conc. (%)	Roughness (mL/min)	Gurley (mL/min)	Contact angle (°)	Whiteness	Gamut volume / 10 ³	Weight gain (g/m ²)
Reference (NS)		329 ± 13	318 ± 7	72 ± 1	162.8 ± 1.3	132 ± 1	1.8 ± 0.3
SB	8	324 ± 14	379 ± 14	75 ± 2	162.3 ± 0.5	146 ± 1	2.5 ± 0.2
	16	311 ± 7	397 ± 4	77 ± 2	164.5 ± 0.3	151 ± 1	1.9 ± 0.2
	24	376 ± 9	420 ± 16	79 ± 1	164.1 ± 0.7	153 ± 1	2.3 ± 0.3
P123	8	368 ± 9	407 ± 6	50 ± 3	165.1 ± 0.2	153.3 ± 0.4	2.9 ± 0.2
	16	379 ± 30	381 ± 5	43 ± 2	165.6 ± 0.2	152 ± 2	2.9 ± 0.1
	24	357 ± 9	354 ± 9	47 ± 1	165.8 ± 0.4	150 ± 2	3.0 ± 0.2
F127	8	378 ± 38	356 ± 5	63 ± 3	163.6 ± 0.6	145 ± 2	2.4 ± 0.2
	16	363 ± 28	325 ± 50	57 ± 1	163.4 ± 0.4	141 ± 3	2.7 ± 0.1
	24	329 ± 18	444 ± 13	53 ± 2	162.2 ± 0.7	150 ± 1	2.7 ± 0.2
PCC	8	414 ± 37	347 ± 5	75 ± 2	160.9 ± 0.3	149 ± 1	2.5 ± 0.3
	16	370 ± 15	381 ± 11	83 ± 2	161.3 ± 0.1	146 ± 1	2.5 ± 0.2
	24	365 ± 5	367 ± 2	80 ± 2	162.5 ± 1.1	143 ± 1	2.7 ± 0.1
P123 (with SB)	8	375 ± 22	376 ± 21	51 ± 3	164.9 ± 1.7	162 ± 3	2.4 ± 0.1
	16	383 ± 36	321 ± 9	48 ± 2	165.4 ± 0.8	161 ± 2	2.8
	24	368 ± 13	374 ± 13	40 ± 3	163.6 ± 0.5	164 ± 2	2.7 ± 0.1

269

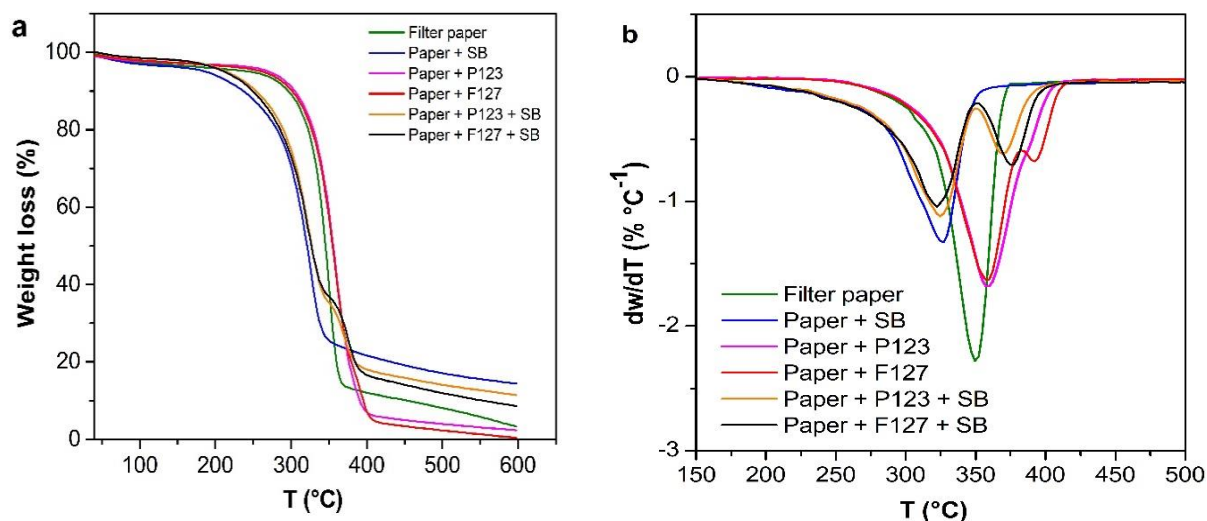
270 In Figure 3b, the GA for different concentrations of Pluronic P123 and F127 is presented. GA is improved by 14.6%
 271 using 8% of P123 in the coating solution; however, the GA is further reduced by increasing the P123 concentration from
 272 8% up to 24%. For F127, the 8% addition improves the GA by 10.5%, but further increase in the concentration of F127,
 273 from 8 up to 16%, reduces the GA as well. However, the use of 24% of F127 showed almost equal GA increase as 24%
 274 of P123, 11.8% and 12.8%, respectively. The increase of GA can be explained by the amphiphilic nature of Pluronic,
 275 which facilitates the strong adsorption of these components on cellulosic surfaces (Liu et al., 2010). Additionally,
 276 Pluronic form inclusive complexes with starches, leading to the formation of self-supporting flocs in the coating
 277 formulation, and enhancing the dispersion of other coating components (Petkova-Olsson et al., 2017; Petkova-Olsson,
 278 Ullsten, & Järnström, 2016). Interestingly enough, the lowest amount of P123 and F127 (8%) was found to be more
 279 favorable to improve GA. This area was also improved by ~7.9% in the presence of PCC at a concentration of 8% or
 280 16% (Figure 3c), which is related to the gain in hydrophobicity of the paper surface. However, roughness increased with
 281 the presence of PCC and GA was further decreased by 3.7% with a large content of PCC (24%) in the coating
 282 formulation.

283 The effect of P123 coatings in combination with SB (16%) and SB (16%)/PCC (16%) is displayed in Figure 3d. It is
 284 observed that GA increases by 8.5-9% using P123 or a mixture of P123 and PCC. It was further improved significantly
 285 by 16-20% and 19-22% with the presence of SB/P123 and SB/P123/PCC, respectively. This increase in GA can be
 286 explained by the sorption of Pluronic on the cellulosic surface, which increases in combination with a highly cationic
 287 polymer (Liu et al., 2011, 2010). Moreover, formation of amylose-Pluronic inclusion complexes may also facilitates the
 288 immobilization of the ink pigments on the coated paper surface, improving GA.

289 TGA contributes to understand the adsorption of Pluronic in the presence of a cationic polymer. Figure 4 (a) and 4 (b)
 290 represent the TGA and DTG curves of dip-coated paper samples, respectively. It can be seen that the major

291 decomposition areas can be divided into three zones, 275 to 350 °C, 300 to 350 °C and 325 to 400 °C for SB coatings,
 292 filter papers and Pluronics coatings, respectively. However, an increase in the major decomposition area of both
 293 Pluronics was observed when filter papers were coated with the presence of SB (+Pluronics), which can be attributed to
 294 an increased adsorption of Pluronics in the presence of SB.

295



296

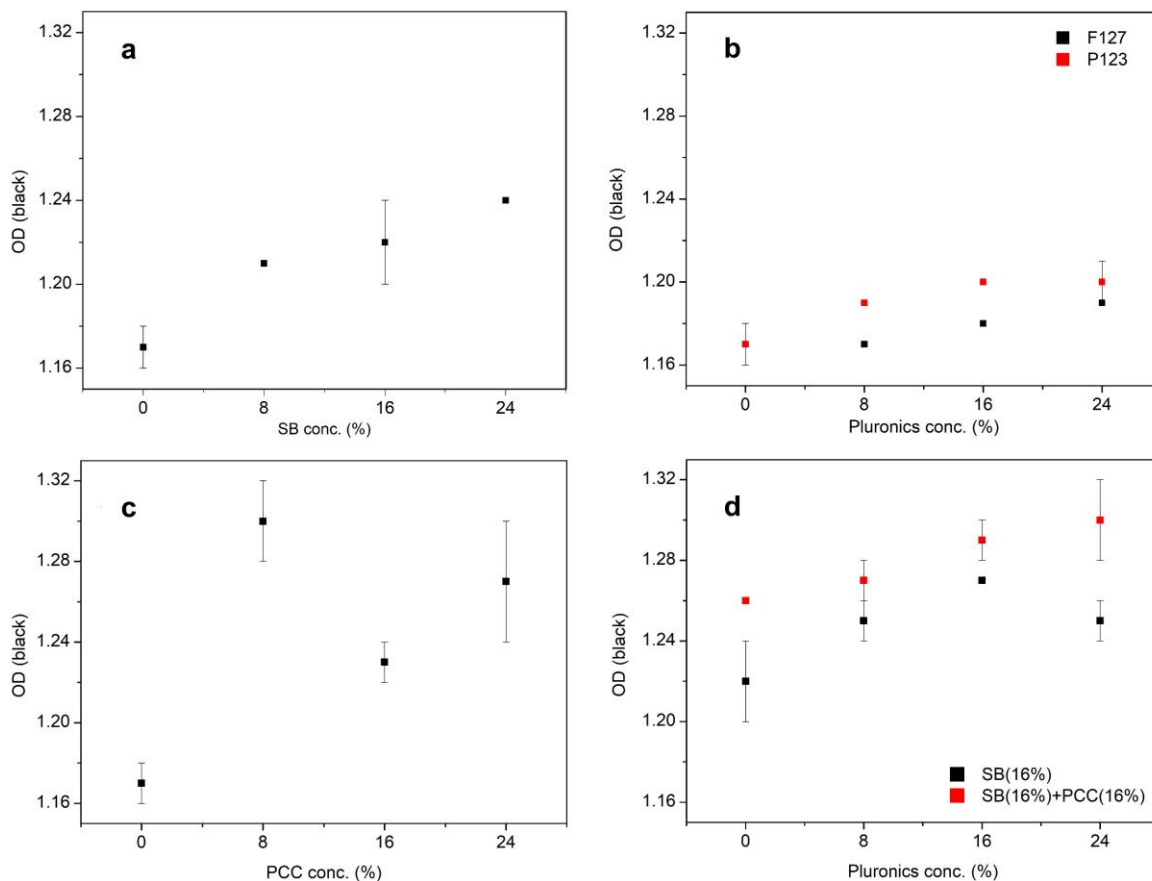
297 Figure 4 TGA (a) and DTG (b) curves for filter paper, paper + SB, paper + P123, paper + F127, paper + P123 + SB and
 298 paper + F127 + SB.

299

300 **Optical density**

301 OD is an important parameter to evaluate the depth of the color tone in the printed papers, which clearly affects the
 302 perceived saturation of a color (Hu, Fu, Chu, & Lin, 2017). Figure 5 represents the OD of the black color with increasing
 303 concentration of SB (A), Pluronics (B), PCC (C) and SB/P123/PCC (D). Figure 5c shows the effect of PCC
 304 concentration on OD. OD for PCC coating correlates with the Gurley permeability, attaining deeper tones as the sheet
 305 became more resistant to air flow (Kasmani, Mahdavi, Alizadeh, Nemati, & Samariha, 2013). The highest improvement
 306 was observed at 8% of PCC. Likewise, OD followed the same trends as GA, and thus it increased with increasing
 307 concentration of SB and P123/F127. Above all, Figure 5d shows that the highest increase in OD was achieved with the
 308 combination of SB-P123-PCC in the coating formulation.

309



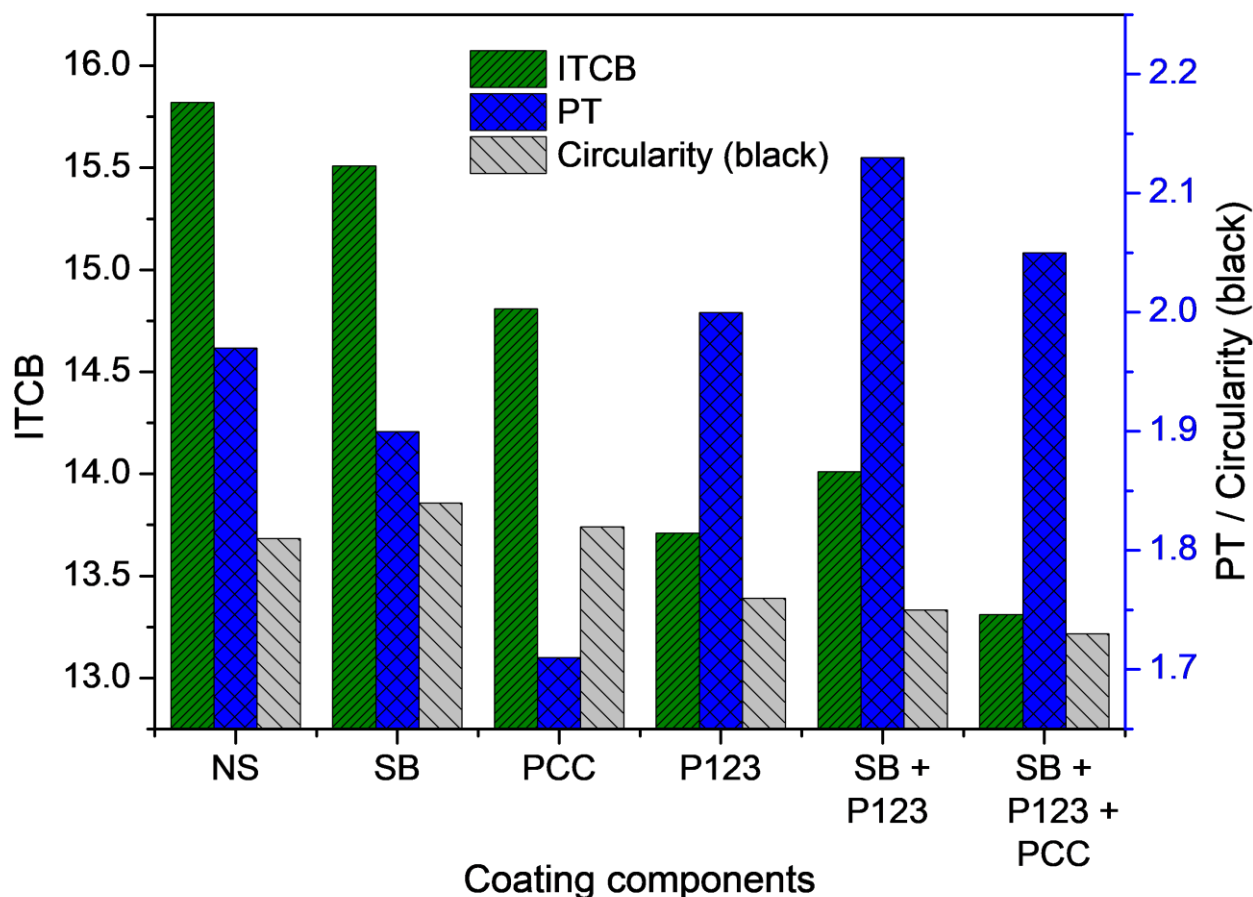
310

311 Figure 5 Effect of different concentrations of SB (a), Pluronics (b), PCC (c) and their combinations (d) on OD (0%:
312 reference coating using NS).

313

314 Inter-color bleed (ITCB), print-through (PT) and circularity for black color

315 Figure 6 presents the ITCB, PT and circularity (black dots) of SB, PCC, P123, SB/P123 and SB/P123/PCC coated
316 papers. Similarly to GA, ITCB was also improved (*i.e.*, reduced) upon the addition of these components. The highest
317 decrease in ITCB, 15.9%, was observed with SB/P123/PCC coatings. Unlike GA and ITCB, PT of SB/P123 or
318 SB/P123/PCC coated paper showed a higher PT at the concentrations used in this work, due to decrease in viscosity of
319 the coating formulation, letting the formulation go deeper into the cellulose matrix, which increased the see-through of
320 ink from the other (non-coated) side of the paper. The presence of PCC on the cellulosic surface provided a better
321 improvement in the PT compared to SB or P123 coated papers. Circularity of black dots generally correlates with the
322 ITCB, improving with the formulation containing SB and P123, due to better fixation of ink particles onto the surface.



323

324 Figure 6 Effect of different coating components on ITCB, PT and circularity of black color.

325

326 Whiteness and fluorescence quenching

327 Whiteness, positively correlated with ISO brightness, represents a paper's ability to equally reflect a balance of all
 328 wavelength of light across the visible spectrum (Hu et al., 2017). The addition of OBA on the paper surface is a cost-
 329 effective solution in papermaking to increase the whiteness of printing and writing papers (Shi et al., 2012). Therefore,
 330 the interaction between OBA and the other coating components is important. From Table 4, it can be noted that the
 331 presence of OBA improved the whiteness of the coated paper but the presence of HCS quenched this agent, resulting in
 332 lower whiteness (Figure S1, Supplementary Information). It is also worth mentioning that the presence of P123 and PCC
 333 did not show any further improvement in the whiteness.

334

335 Table 4 Study of interactions among factors. Percentages are related to the total solids content (on the basis of dry
 336 weight) of coating formulations.

HCS (%)	P123 (%)	PCC (%)	OBA (%)	GA	OD (cyan)	OD (Magenta)	OD (yellow)	OD (black)	PT	ITCB	Circularity (Black)	Whiteness
0	0	0	0	6512	0.76	0.87	1.31	1.23	1.6	15.5	1.95	146
0	0	0	6	6301	0.74	0.84	1.31	1.17	1.97	15.8	1.81	162
0	0	16	0	6596	0.76	0.88	1.33	1.20	1.56	15.4	1.98	146

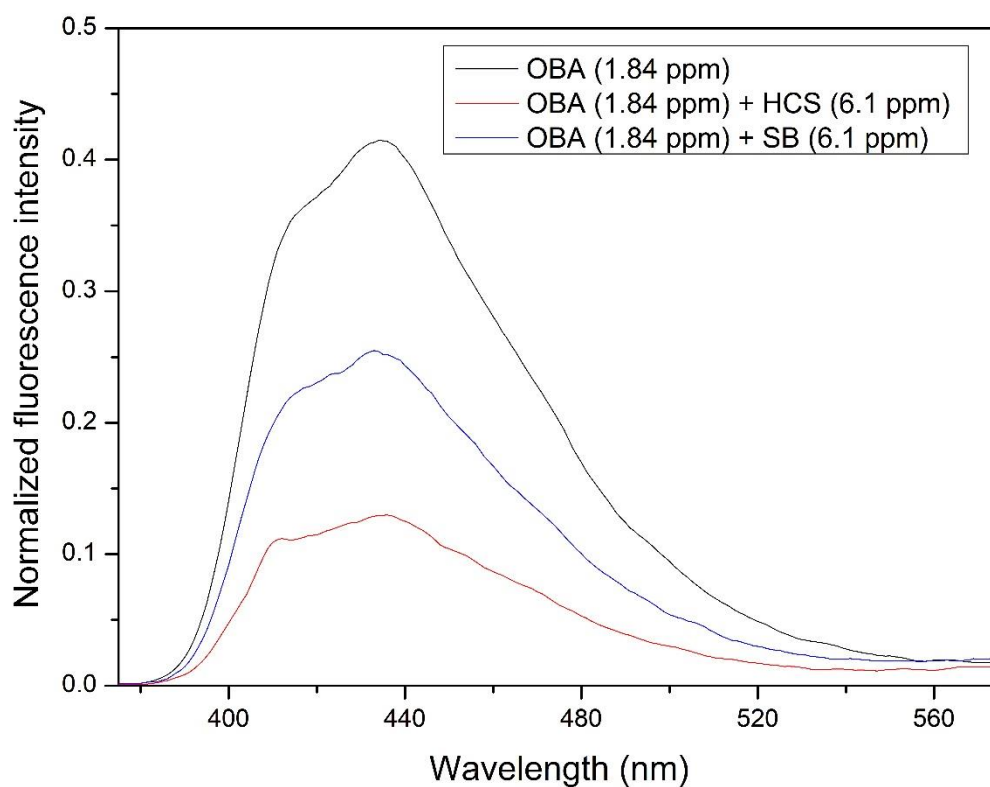
0	0	16	6	7074	0.80	0.91	1.36	1.21	1.76	14.4	1.81	162
0	16	0	0	6758	0.79	0.89	1.33	1.22	1.76	14.5	1.80	146
0	16	0	6	6922	0.80	0.90	1.34	1.20	1.86	13.7	1.76	162
0	16	16	0	7004	0.81	0.90	1.34	1.20	1.80	14.2	1.74	146
0	16	16	6	6802	0.81	0.90	1.33	1.21	1.69	14.0	1.71	163
8	8	8	3	7122	0.82	0.90	1.34	1.19	1.65	13.8	1.80	148
8	8	8	3	7212	0.82	0.91	1.33	1.20	1.69	14.2	1.81	147
16	0	0	0	6610	0.80	0.78	1.33	1.25	1.99	16.0	1.79	144
16	0	0	6	6656	0.74	0.77	1.37	1.24	1.78	16.2	1.79	145
16	0	16	0	6971	0.77	0.88	1.31	1.20	1.82	15.6	1.95	144
16	0	16	6	6739	0.79	0.78	1.31	1.23	1.82	15.6	1.84	146
16	16	0	0	7479	0.83	0.92	1.36	1.22	1.80	12.7	1.83	146
16	16	0	6	7443	0.86	0.85	1.50	1.42	1.66	16.3	1.89	146
16	16	16	0	7427	0.83	0.91	1.35	1.20	1.72	13.9	1.76	145
16	16	16	6	7670	0.85	0.93	1.37	1.22	1.84	13.2	1.71	148

337

338 In comparison to NS coatings, whiteness increased by 11% with the addition of OBA. As aforementioned, HCS (with
339 OBA) reduced the whiteness of coated papers by ~10.85% due to the OBA quenching, irrespective of the presence of
340 any other components. Interestingly, such loss of whiteness was not observed when SB was used instead of the cationic
341 starch ether (Figure S1).

342 To understand the OBA quenching effect in the presence of HCS and SB, fluorescence emission spectra were recorded
343 for solutions containing OBA (1.84 ppm) and either cationic starch (6.1 ppm), so as to keep the same ratio as in coating
344 formulations (6% OBA / 16% CS). Fluorescence quenching was clear in the presence of all cationic starches but, in the
345 case of HCS, the intensity of the emission of blue light (~440 nm) decreased almost by a factor of 4 (Figure 7).

346 Quenching was possibly due to the formation of a non-fluorescent complex, where the sulfonate groups of OBA donate
347 electrons to the quaternary ammonium groups of HCS. Still, the most plausible explanation is the aggregation-caused
348 quenching, where aggregation is promoted by electrostatic interactions. The reason for this is that solutions at higher
349 concentration, such as 9.2 ppm OBA / 24.4 ppm HCS, showed Rayleigh scattering to such extent that no reliable
350 spectrum could be obtained, even though a concentration of 24.4 ppm lies much below the solubility limit of HCS. In
351 other words, there was a phase transition from solution to dispersion when both solutions, each of them displaying
352 negligible light scattering, were mixed. However, regardless of the quenching mechanism, neither this aggregation nor
353 that extent of quenching was observed when using SB/OBA at the same concentrations, supporting the previously
354 described retention of paper whiteness. Given that SB and HCS had the same DS, it may be concluded that the cationic
355 starch ester possesses a key advantage over its ether counterpart. This advantage should, undoubtedly, be further
356 explored.



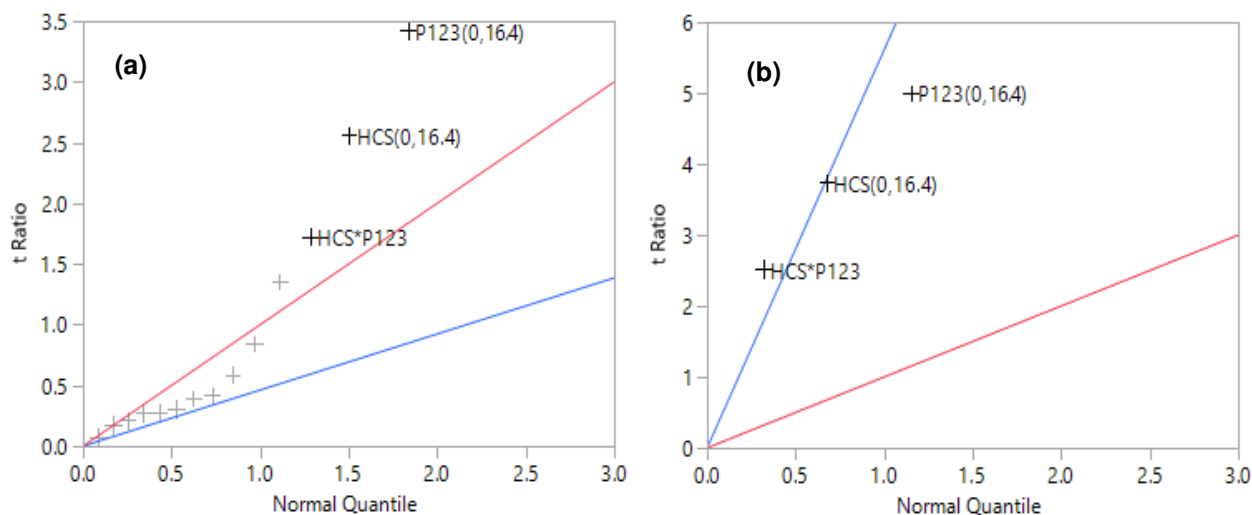
357
 358 Figure 7 Fluorescence emission spectrum of OBA in presence of HCS and SB. An excitation wavelength of 350 nm was
 359 used to record all spectrum.

360

361 **Statistical analysis**

362 Figures 8a and 8b show the half-normal plots, as obtained from JMP software, for all the studied factors. As indicated in
 363 Figure 8a, three major factors are clearly falling off from the red straight line. In other words, P123, HCS and their
 364 interaction (HCS*P123) can be considered as the most significant factors to affect the GA, whereas PCC and OBA, like
 365 their interaction, were found to be insignificant. The model was further optimized through prediction plots and ANOVA
 366 study, and insignificant factors were removed. Figure 8b indicates the half-normal plot of the model, considering only
 367 the significant factors.

368



369
370 Figure 8 Half-normal plot for gamut area: a) considering all factors; b) considering only significant factors.

371
372 A prediction profile for GA and a complete report of the model is provided in the Supplementary Information. From this
373 statistical study, it can be inferred that the combination of HCS and Pluronic in the coating formulation, together with
374 the presence of PCC and OBA, led to improve the printability of coated papers. The statistical study of these
375 components has shown that, for GA, the incorporation of P123, the presence of HCS and their interaction, have
376 significant effect in the selected range. Regarding the most important variables for the other printing properties, P123
377 has significant effect on OD for cyan/magenta/yellow and on ITCB, whereas HCS impacts OD of black color. The
378 ternary interaction HCS-P123-OBA showed a good impact on PT (not seen with SB-P123-OBA) and the binary
379 interaction P123-PCC affects the circularity of black color. The corresponding half-normal plot, the analysis of variance
380 and the prediction profiles have also been included in the Supplementary Information. All considered, the combination
381 of both HCS and P123, accounting for a total solids content of 16%, has the greatest impact on the overall printing
382 quality.

383

384 Conclusions

385 The effect of an unconventional combination of coating components, highly substituted cationic starch and Pluronic, on
386 the printing quality of office papers was investigated. As a key novelty, cationic starch refers not only to its typical ether
387 form, but also to starch betainate, an ester that has been suggested for bulk addition in sheet forming but not (as far as
388 the authors are concerned) for paper coating. A 24% coating weight of starch betainate increased the gamut area by
389 12.5%, whilst Pluronic P123 and F127 (8% coating weight) attain improvements of 14.6% and 11.8%, respectively.
390 Both cationic starches, ether and ester, showed the same outcome for improving the paper printing properties in presence
391 and absence of Pluronic. Nonetheless, while the ether caused a certain loss of whiteness, as it quenches the fluorescence
392 emission of the optical agent, such loss was not found when starch betainate was used. The ability of starch betainate of
393 keeping the whiteness gain of an anionic brightening agent is a key finding of this work.

394 Remarkably, the statistical analysis indicated that besides the aforementioned individual effects of cationic starch and
395 Pluronic, the binary interaction thereof had a significantly positive influence on the gamut area. Furthermore, the
396 optical density (cyan, magenta, yellow and black), print-through, inter-color bleed and circularity were successfully
397 correlated with the independent variables. It was shown, for instance, that the print-through was significantly affected by
398 the presence of conventional cationic starch, OBA and Pluronic P123.

399

400 **Declarations**

401 **Funding**

402 This work was carried out under the Project in pactus -innovative products and technologies from eucalyptus, Project N.º
403 21874 funded by Portugal 2020 through European Regional Development Fund (ERDF) in the frame of COMPETE
404 2020 nº246/AXIS II/2017. Authors would like to thank the Coimbra Chemical Centre, which is supported by the
405 Fundação para a Ciência e a Tecnologia (FCT), through the projects UID/QUI/00313/2020 and COMPETE. Authors
406 would also like to thank the CIEPQPF - Strategic Research Centre Project UIDB/00102/2020, funded by the Fundação
407 para a Ciência e Tecnologia (FCT). M.S. acknowledges the PhD grant BDE 03|POCI-01-0247-FEDER-021874. R.A.
408 acknowledges the post-doc grant BPD 02|POCI-01-0247-FEDER-021874.

409 **Conflicts of interest/Competing interests**

410 The authors declare that there is no conflict of interest and that they do not have competing interests.

411 **Availability of data and material**

412 All data are displayed in the article and its electronic supplementary information.

413 **Code availability**

414 Not applicable.

415 **Authors' contributions**

416 All authors made substantial contributions to the conception of the work, the acquisition and interpretation of data, and
417 writing. All authors approve the manuscript. All authors agree to be accountable for all aspects of the work in ensuring
418 that questions related to the accuracy or integrity of any part of the work are appropriately investigated and resolved.

419 **Ethics approval**

420 Not applicable. No studies involving humans and/or animals.

421 **Consent to participate**

422 Not applicable. No studies involving humans and/or animals.

423 **Consent for publication**

424 Not applicable. No studies involving humans and/or animals.

425

426 **References**

- 427 Alexandridis, P., Holzwarth, J. F., & Hatton, T. A. (1994). Micellization of Poly(ethylene oxide)-Poly(propylene
428 oxide)-Poly(ethylene oxide) Triblock Copolymers in Aqueous Solutions Thermodynamics of copolymer
429 Association. *Macromolecules*, 27, 2414–2425.
- 430 Auzély-Velty, R., & Rinaudo, M. (2003). Synthesis of starch derivatives with labile cationic groups. *International
431 Journal of Biological Macromolecules*, 31(4–5), 123–129.
- 432 Baptista, J. G. C., Rodrigues, S. P. J., Matsushita, A. F. Y., Vitorino, C., Maria, T. M. R., Burrows, H. D., ... Valente, A.
433 J. M. (2016). Does poly(vinyl alcohol) act as an amphiphilic polymer? An interaction study with simvastatin.
434 *Journal of Molecular Liquids*, 222, 287–294.
- 435 Bendoraitiene, J., Lekniute-Kyzike, E., & Rutkaite, R. (2018). Biodegradation of cross-linked and cationic starches.
436 *International Journal of Biological Macromolecules*, 119, 345–351.
- 437 Bollström, R., Tobjörk, D., Dolietis, P., Salminen, P., Preston, J., Österbacka, R., & Toivakka, M. (2013). Printability of
438 functional inks on multilayer curtain coated paper. *Chemical Engineering and Processing: Process Intensification*.
439 <https://doi.org/10.1016/j.cep.2012.07.007>
- 440 Gao, J., Luo, Z., Fu, X., Luo, F., & Peng, Z. (2012). Effect of enzymatic pretreatment on the synthesis and properties of
441 phosphorylated amphoteric starch. *Carbohydrate Polymers*, 88(3), 917–925.
442 <https://doi.org/10.1016/j.carbpol.2012.01.034>
- 443 Gigac, J., Stankovská, M., Opálená, E., & Pažitný, A. (2016). The effect of Pigments and Binders on Inkjet Print
444 Quality. *Wood Research*, 61(2), 215–226.
- 445 Gigac, J., Stankovska, M., & Pazitny, A. (2016). Influence of the Coating Formulations and Base Papers on Inkjet
446 Printability. *Wood Research*, 61(6), 915–926.
- 447 Granö, H., Yli-Kauhaluoma, J., Suortti, T., Käki, J., & Nurmi, K. (2000). Preparation of starch betainate: a novel
448 cationic starch derivative. *Carbohydrate Polymers*, 41(3), 277–283.
- 449 Haack, V., Heinze, T., Oelmeyer, G., & Kulicke, W. M. (2002). Starch derivatives of high degree of functionalization, 8
450 synthesis and flocculation behavior of cationic starch polyelectrolytes. *Macromolecular Materials and
451 Engineering*, 287(8), 495–502.
- 452 He, Z., & Alexandridis, P. (2018). Micellization thermodynamics of Pluronic P123 (EO20PO70EO20) amphiphilic
453 block copolymer in aqueous Ethylammonium nitrate (EAN) solutions. *Polymers*, 10(32).
- 454 Hebeish, A., Higazy, A., El-Shafei, A., & Sharaf, S. (2010). Synthesis of carboxymethyl cellulose (CMC) and starch-
455 based hybrids and their applications in flocculation and sizing. *Carbohydrate Polymers*, 79(1), 60–69.
- 456 Hu, G., Fu, S., Chu, F., & Lin, M. (2017). Relationship between paper whiteness and color reproduction in inkjet
457 printing. *BioResources*, 12(3), 4854–4866. <https://doi.org/10.15376/biores.12.3.4854-4866>
- 458 Huber, K. C., & BeMiller, J. N. (2001). Location of sites of reaction within starch granules. *Cereal Chemistry*, 78(2),
459 173–180. <https://doi.org/10.1094/CCHEM.2001.78.2.173>
- 460 Kasmani, J. E., Mahdavi, S., Alizadeh, A., Nemati, M., & Samariha, A. (2013). Physical properties and printability
461 characteristics of mechanical printing paper with LWC. *BioResources*, 8(3), 3646–3656.
462 <https://doi.org/10.15376/biores.8.3.3646-3656>
- 463 Lamminmäki, T. T., Kettle, J. P., & Gane, P. A. C. (2011). Absorption and adsorption of dye-based inkjet inks by
464 coating layer components and the implications for print quality. *Colloids and Surfaces A: Physicochemical and
465 Engineering Aspects*, 380(1–3), 79–88.
- 466 Lee, H. L., Shin, J. Y., Koh, C.-H., Ryu, H., Lee, D.-J., & Sohn, C. (2002). Surface sizing with cationic starch: its effect
467 on paper quality and the papermaking process. *Tappi Journal*, 1(1), 34–40.
- 468 Liu, X., Vesterinen, A. H., Genzer, J., Seppälä, J. V., & Rojas, O. J. (2011). Adsorption of PEO-PPO-PEO triblock
469 copolymers with end-capped cationic chains of poly(2-dimethylaminoethyl methacrylate). *Langmuir*.

470 <https://doi.org/10.1021/la201596x>
471 Liu, X., Wu, D., Turgman-Cohen, S., Genzer, J., Theyson, T. W., & Rojas, O. J. (2010). Adsorption of a nonionic
472 symmetric triblock copolymer on surfaces with different hydrophobicity. *Langmuir*.
473 <https://doi.org/10.1021/la100156a>
474 Lourenço, A. F., Gamelas, J. A. F., Sarmiento, P., & Ferreira, P. J. T. (2020). Cellulose micro and nanofibrils as coating
475 agent for improved printability in office papers. *Cellulose*, 27(10), 6001–6010. [https://doi.org/10.1007/s10570-](https://doi.org/10.1007/s10570-020-03184-9)
476 [020-03184-9](https://doi.org/10.1007/s10570-020-03184-9)
477 Lundberg, A., Örtengren, J., Norberg, O., & Wågberg, K. (2010). Improved print quality by surface fixation of pigments.
478 *International Conference on Digital Printing Technologies*, (February), 251–255.
479 Niegelhell, K., Chemelli, A., Hobisch, J., Griesser, T., Reiter, H., Hirn, U., & Spirk, S. (2018). Interaction of industrially
480 relevant cationic starches with cellulose. *Carbohydrate Polymers*, 179, 290–296.
481 Petkova-Olsson, Y., Altun, S., Ullsten, H., & Järnström, L. (2017). Temperature effect on the complex formation
482 between Pluronic F127 and starch. *Carbohydrate Polymers*, 166, 264–270.
483 Petkova-Olsson, Y., Ullsten, H., & Järnström, L. (2016). Thermosensitive silica-pluronic-starch model coating
484 dispersion-part I: The effect of Pluronic block copolymer adsorption on the colloidal stability and rheology.
485 *Colloids and Surfaces A: Physicochemical and Engineering Aspects*, 506, 245–253.
486 <https://doi.org/10.1016/j.colsurfa.2016.06.032>
487 Sharma, M., Aguado, R., Murtinho, D., Valente, A. J. M., & Ferreira, P. J. T. (2021). International Journal of Biological
488 Macromolecules Novel approach on the synthesis of starch betainate by transesterification. *International Journal*
489 *of Biological Macromolecules*, 182, 1681–1689. <https://doi.org/10.1016/j.ijbiomac.2021.05.175>
490 Sharma, M., Aguado, R., Murtinho, D., Valente, A. J. M., Mendes De Sousa, A. P., & Ferreira, P. J. T. (2020, November
491 1). A review on cationic starch and nanocellulose as paper coating components. *International Journal of*
492 *Biological Macromolecules*, Vol. 162, pp. 578–598. <https://doi.org/10.1016/j.ijbiomac.2020.06.131>
493 Shi, H., Liu, H., Ni, Y., Yuan, Z., Zou, X., & Zhou, Y. (2012). Review: Use of optical brightening agents (OBAs) in the
494 production of paper containing high-yield pulps. *BioResources*, 7(2), 2582–2591.
495 <https://doi.org/10.15376/biores.7.2.2582-2591>
496 Sousa, S., De Sousa, A. M., Reis, B., & Ramos, A. (2014). Influence of Binders on Inkjet Print Quality. *Materials*
497 *Science*, 20(1). <https://doi.org/10.5755/j01.ms.20.1.1998>
498 Stankovská, M., Gigac, J., Letko, M., & Opálená, E. (2014). The Effect of Surface Sizing on Paper Wettability and on
499 Properties of Inkjet Prints. *Wood Research*, 59(1), 67–76.
500 Thapa, R. K., Cazzador, F., Grønlien, K. G., & Tønnesen, H. H. (2020). Effect of curcumin and cosolvents on the
501 micellization of Pluronic F127 in aqueous solution. *Colloids and Surfaces B: Biointerfaces*, 195(July 2020).
502 <https://doi.org/10.1016/j.colsurfb.2020.111250>
503 Wang, S., & Cheng, Q. (2009). A novel process to isolate fibrils from cellulose fibers by high-intensity ultrasonication,
504 Part 1: Process optimization. *Journal of Applied Polymer Science*, 113(2), 1270–1275.
505

Supplementary Files

This is a list of supplementary files associated with this preprint. Click to download.

- [supplementarymaterial.doc](#)